

# ***WW* Scattering in the Era of Post Higgs Discovery**

Jung Chang<sup>1</sup>, Kingman Cheung<sup>1,2</sup>, Chih-Ting Lu<sup>1</sup>, Tzu-Chiang Yuan<sup>3</sup>

<sup>1</sup> *Department of Physics, National Tsing Hua University, Hsinchu 300, Taiwan*

<sup>2</sup> *Division of Quantum Phases and Devices, School of Physics,  
Konkuk University, Seoul 143-701, Republic of Korea*

<sup>3</sup> *Institute of Physics, Academia Sinica, Nangang, Taipei 11529, Taiwan*

(Dated: March 27, 2013)

## Abstract

More evidences have now been collected at the Large Hadron Collider suggesting the new 125~126 GeV boson is likely the long sought Higgs boson in the standard model. One pressing question continued being asked by theorists is whether this Higgs boson is a lone player responsible for the full electroweak symmetry breaking. Current data still allow room for additional Higgs bosons or some other UV physics that may play a partial role in electroweak symmetry breaking as well. We use the *WW* scattering to investigate such a possibility, using the two-Higgs-doublet model as a prototype. The *WW* scattering becomes strong when the extra Higgs bosons are very heavy. We study the sensitivity of the *partially strong WW* scattering signals at the 13 TeV Large Hadron Collider.

PACS numbers: 14.80.Bn, 14.80.Cp, 12.60.Fr, 12.15.Ji

## I. INTRODUCTION

A new particle with mass of 125~126 GeV was discovered at the Large Hadron Collider (LHC) in July 2012 [1, 2]. This may be the long sought Higgs boson of the standard model (SM), which was proposed in 1960s [3], or one of the Higgs bosons beyond the SM. For example, supersymmetric theories, little-Higgs models, and other extended Higgs sector such as the two-Higgs-doublet models (2HDM) all contain a multitude of neutral as well as charged Higgs bosons. The current data still contain large uncertainties that these various extensions of the SM cannot be confirmed or ruled out decisively. Based on the data on the signal strengths of all decay channels of the Higgs boson, it is therefore important to constrain various couplings of the Higgs boson. Indeed, several precision studies of the Higgs boson appeared recently, either in model-independent approach [4] or in specific models (e.g., two-Higgs-doublet models [5]).

One of the most useful constraints from the global fitting of the Higgs boson couplings is the one to a pair of  $W/Z$  bosons. The current data constrain [4]

$$C_v \equiv \frac{g_{hWW}}{g_{hWW}^{\text{SM}}} = 0.96^{+0.13}_{-0.15} . \quad (1)$$

The central value is close to 1, which means that the observed Higgs boson leaves only little room for the existence of another Higgs boson or some unknown UV physics responsible for the electroweak symmetry breaking (EWSB). If  $C_v$  is exactly equal to 1, it means that the observed Higgs boson will completely account for the EWSB. We do not need another Higgs boson, or if another Higgs boson exists it has nothing to do with the EWSB, for example in the inert Higgs doublet model. Nevertheless, it is not unreasonable that the value of  $C_v$  could deviate from the central value by  $-2\sigma$ , then the  $C_v$  could be as low as 0.66. One certainly needs more data to reduce the error.

If the  $hWW$  coupling is less than its SM value, there must be something heavier, could be as heavy as a few TeV, to complete the EWSB. The simplest realization of this scenario is the 2HDM, in which the light CP-even Higgs boson  $h$  is at 125-126 GeV while the heavy CP-even Higgs boson  $H$  is at 1-2 TeV. These two CP-even Higgs bosons couple to the vector boson with reduced strengths  $g_{hWW} = \sin(\beta - \alpha)g_{hWW}^{\text{SM}}$  and  $g_{HWW} = \cos(\beta - \alpha)g_{hWW}^{\text{SM}}$  such that  $g_{hWW}^2 + g_{HWW}^2 = (g_{hWW}^{\text{SM}})^2$ , where  $\tan\beta$  is the ratio of the VEVs of the two doublets and  $\alpha$  the mixing angle between the two CP-even neutral Higgs bosons. At low energy only one light CP-even Higgs boson is relevant. One can then parametrize all the UV effects with

all the heavier Higgs bosons being integrated out by an effective Lagrangian as presented in Ref.[6].

As is well known, scattering of the longitudinal components of the weak gauge bosons is a useful probe of the EWSB sector [7, 8]. The scattering amplitudes with purely gauge contributions grow with energy as  $s/m_W^2$ , where  $s$  is the squared center-of-mass (CM) energy of the  $W_L W_L$  system. In the SM with a light Higgs boson, the amplitude will be completely unitarized by the Higgs boson. Once  $\sqrt{s}$  goes beyond the light Higgs boson mass, the scattering amplitude will no longer grow like  $s/m_W^2$ . On the other hand, if the  $hWW$  coupling deviates from the SM value, even by a small amount, the terms growing like  $s/m_W^2$  in the scattering amplitude would become strong after hitting the light Higgs pole. Furthermore, if the scale of the UV part is far enough from the light Higgs boson, the onset of strong  $W_L W_L$  scattering between the light Higgs mass and the UV scale should be discernible at the LHC, as was demonstrated for a generic extended Higgs sector in [9] as well as for an extra hidden  $Z'$  model in [10]. This temporal growth of  $W_L W_L$  scattering amplitudes in the immediate range of energy is of immense interests to the LHC experiments, in particular with its upgrade to 13-14 TeV. Previously, the calculation was done using the naive effective  $W$  approximation [11]. In this work, we extend our previous work [9] to include the full calculations with detector simulations.

In the full calculation of  $qq \rightarrow qqW^+W^-$ , there are (i) vector-boson fusion (VBF) diagrams and (ii) non-VBF diagrams, e.g., the  $W$  bosons simply radiate off the external quark legs. The non-VBF diagrams do not involve the dynamics in the EWSB sector, and thus should be suppressed by devising appropriate kinematical cuts. The  $WW$  fusion can be extracted by the presence of two energetic forward jets. We can impose selection cuts to select jets in forward rapidity and high energy region [12]. Furthermore, if we demand the leptonic decay of the vector bosons, there will be very few jet activities in the central rapidity region [13]. Previous studies in the context of strongly interacting EWSB sector were performed in Ref. [14]. Similar selection cuts can be applied here for partially strong  $W_L W_L$  scattering.

The organization of this paper is as follows. In Sec. II, we first briefly review some details how the bad energy behavior in the  $W_L W_L$  scattering amplitudes in SM is completely cancelled among the gauge and Higgs diagrams. We then discuss how the modified gauge-Higgs coupling may lead to incomplete cancellation and thus the partial growth in the scattering amplitudes in the intermediate energy range. Using the 2HDM as an illustration

we present our numerical results to support this partially strong  $W_L W_L$  scattering for the 13 TeV LHC in Sec. III. We conclude in Sec. IV.

Note that the use of the 2HDM is only for simplicity and renormalizability. The main point here is that the model could account for the light CP-even Higgs boson observed at the LHC. This Higgs boson is partially responsible for the EWSB and the other part of the EWSB is rather heavy. The 2HDM has at least six independent free parameters and certainly has enough freedom to allow us to implement this scenario. We are looking at the window between this light Higgs boson and the heavy UV part where the  $W_L W_L$  scattering may reveal the nature of the EWSB sector at the LHC.

A previous work on using  $WW$  scattering to investigate the anomalous  $g_{hWW}$  coupling can be found in Ref. [15]. Another interesting approach is to determine the relative longitudinal to transverse production of the vector bosons by measuring the polarization of the vector bosons [16].

## II. $WW$ SCATTERING AMPLITUDES

Let us begin by recalling the derivation of a covariant form for the longitudinal polarization 4-vector  $\epsilon_L^\mu(p)$  of the vector boson, say the  $W$  boson. The leading piece is directly proportional to  $p^\mu/m_W$ . We can write it as

$$\epsilon_L^\mu(p) = p^\mu/m_W + v^\mu(p) \quad (2)$$

with

$$v^\mu(p) \simeq -\frac{m_W}{2p^0} (p^0, -\vec{p}) \sim O(m_W/E_W). \quad (3)$$

Since this form of  $v^\mu$  is not covariant, so the calculation involving  $v^\mu$  would be cumbersome. Nevertheless, in the center-of-mass frame of the incoming  $W^+(p_1)W^-(p_2)$  pair, where  $\vec{p}_1 = -\vec{p}_2$ , we can express

$$v^\mu(p_1) = -\frac{2m_W}{s} p_2^\mu \quad (4)$$

and so the polarization 4-vector  $\epsilon_L^\mu(p_1)$  can be expressed as

$$\epsilon_L^\mu(p_1) = \frac{p_1^\mu}{m_W} - \frac{2m_W}{s} p_2^\mu \quad (5)$$

and similarly

$$\epsilon_L^\mu(p_2) = \frac{p_2^\mu}{m_W} - \frac{2m_W}{s} p_1^\mu \quad (6)$$

where  $s = (p_1 + p_2)^2$ . For outgoing  $W^+(k_1)W^-(k_2)$  pair, simply make the substitution of  $(p_1, p_2) \rightarrow (k_1, k_2)$  to obtain the covariant form for their polarization vectors.

Next consider the process  $W^+(p_1)W^-(p_2) \rightarrow W^+(k_1)W^-(k_2)$ , which has contributing Feynman diagrams of  $\gamma, Z$  in both  $s$  and  $t$  channels and a 4-point vertex, as well as the Higgs boson exchange in  $s$  and  $t$  channels. The amplitudes for the gauge diagrams are given by

$$\begin{aligned}
i\mathcal{M}_t^{\gamma+Z} &= -ig^2 \left( \frac{s_W^2}{t} + \frac{c_W^2}{t - m_Z^2} \right) [(p_1 + k_1)^\mu \epsilon(p_1) \cdot \epsilon(k_1) - 2k_1 \cdot \epsilon(p_1) \epsilon^\mu(k_1) - 2p_1 \cdot \epsilon(k_1) \epsilon^\mu(p_1)] \\
&\quad \times [(p_2 + k_2)_\mu \epsilon(p_2) \cdot \epsilon(k_2) - 2k_2 \cdot \epsilon(p_2) \epsilon_\mu(k_2) - 2p_2 \cdot \epsilon(k_2) \epsilon_\mu(p_2)] \quad , \\
i\mathcal{M}_s^{\gamma+Z} &= -ig^2 \left( \frac{s_W^2}{s} + \frac{c_W^2}{s - m_Z^2} \right) [(p_1 - p_2)^\mu \epsilon(p_1) \cdot \epsilon(p_2) + 2p_2 \cdot \epsilon(p_1) \epsilon^\mu(p_2) - 2p_1 \cdot \epsilon(p_2) \epsilon^\mu(p_1)] \\
&\quad \times [(k_2 - k_1)_\mu \epsilon(k_1) \cdot \epsilon(k_2) - 2k_2 \cdot \epsilon(k_1) \epsilon_\mu(k_2) + 2k_1 \cdot \epsilon(k_2) \epsilon_\mu(k_1)] \quad , \\
i\mathcal{M}_4 &= ig^2 [2\epsilon(p_2) \cdot \epsilon(k_1) \epsilon(p_1) \cdot \epsilon(k_2) - \epsilon(p_2) \cdot \epsilon(p_1) \epsilon(k_1) \cdot \epsilon(k_2) - \epsilon(p_2) \cdot \epsilon(k_2) \epsilon(p_1) \cdot \epsilon(k_1)] \quad .
\end{aligned}$$

Substituting the form of the longitudinal polarization vectors into the above amplitudes, the leading term of order  $O(E^4/m_W^4)$  of each amplitude is

$$\begin{aligned}
i\mathcal{M}_t^{\gamma+Z} &= -i \frac{g^2}{4m_W^4} \left[ (s - u)t - 3m_W^2(s - u) + \frac{8m_W^2}{s} u^2 \right] \quad , \\
i\mathcal{M}_s^{\gamma+Z} &= -i \frac{g^2}{4m_W^4} \left[ s(t - u) - 3m_W^2(t - u) \right] \quad , \\
i\mathcal{M}_4 &= i \frac{g^2}{4m_W^4} \left[ s^2 + 4st + t^2 - 4m_W^2(s + t) - \frac{8m_W^2}{s} ut \right] \quad .
\end{aligned}$$

The gauge structure ensures that the cancellation of  $O(E^4/m_W^4)$  terms<sup>1</sup>. The sum of the gauge diagrams are left with terms proportional to  $O(E^2/m_W^2)$ :

$$i\mathcal{M}^{\text{gauge}} = i\mathcal{M}_t^{\gamma+Z} + i\mathcal{M}_s^{\gamma+Z} + i\mathcal{M}_4 = -i \frac{g^2}{4m_W^2} u + O((E/m_W)^0) \quad .$$

Suppose the  $hWW$  coupling is merely a fraction  $C_v$  of its SM value as defined in Eq.(1).

The contributions from the Higgs diagrams are

$$\begin{aligned}
i\mathcal{M}^{\text{Higgs}} &= -i \frac{C_v^2 g^2}{4m_W^2} \left[ \frac{(s - 2m_W^2)^2}{s - m_h^2} + \frac{(t - 2m_W^2)^2}{t - m_h^2} \right] \quad , \\
&\simeq i \frac{C_v^2 g^2}{4m_W^2} u \quad , \tag{7}
\end{aligned}$$

---

<sup>1</sup> In an extra hidden  $Z'$  model, it has been shown in [10] that even the  $O(E^4/m_W^4)$  terms are not cancelled and may lead to partially strong  $W_L W_L$  scattering as well.

in the limit of  $s \gg m_h^2, m_W^2$ . Only if  $C_v$  is exactly equal to 1 as in SM can the bad energy-growing term be delicately cancelled between the gauge diagrams and the Higgs diagrams. Historically an upper bound of the SM Higgs mass of  $m_h^2 < 4\pi\sqrt{2}/G_F$  was first deduced based on the unitarity constraint on the  $W_L W_L$  scattering [7]. Nowadays more useful theoretical lower and upper bounds for the Higgs mass  $129 < m_h(\text{GeV}) < 180$  can be obtained by considering the vacuum stability [17] and perturbativity [18] of the SM scalar potential. Nevertheless, back to our own track. In some extended models that the light Higgs boson has only a fraction of the SM coupling strength (i.e.  $C_v < 1$ ), one expects the total scattering amplitude to keep growing with  $s$  after hitting the light Higgs pole at 125-126 GeV. We expect the UV part of the EWSB sector will come in eventually to unitarize the amplitude at sufficiently high energy to restore unitarity. It was shown that the violation of unitarity occurs at  $\sqrt{s_{WW}} = 1.2, 1.7, 2.7, 3.8$  TeV for a modified  $hWW$  coupling with  $C_v = 0, 0.71, 0.89, 0.95$ , respectively [9].

As alluded already in the introduction, the simplest realization of the above scenario of temporal growth of  $W_L W_L$  scattering amplitude is the 2HDM, in which  $C_v$  is given by  $\sin(\beta - \alpha)$ . The heavier neutral Higgs boson couples to the weak gauge boson with a reduced strength  $g_{HWW} = \cos(\beta - \alpha)g_{HWW}^{\text{SM}}$  such that it can unitarize the rest of the growing amplitudes when  $s_{WW} > m_H^2$ . We will use this scenario in 2HDM to investigate the sensitivity at the LHC.

### III. EXPERIMENTAL CUTS FOR VBF AND NUMERICAL RESULTS

The central issue for the experimental detection of  $WW$  scattering is to separate the VBF diagrams among all the other non-VBF ones. In the VBF diagrams, each of the initial quarks radiates a  $W/Z$  boson, which further scatters into the final state  $W/Z$  bosons. The unique feature of this process is that the scattered quark is very energetic, carrying almost all the energy of the incoming quark and very forward [12, 13]. Furthermore, if we demand the leptonic decays of the  $W$  and  $Z$  bosons, there will be very little hadronic activities in the central rapidity region. Therefore, the signature includes (i) the appearance of two energetic forward jets with large spatial separation, and (ii) the leptonic decay products of the  $W$  or  $Z$  bosons are enhanced at the large invariant mass region.

Based on these features we impose the following experimental cuts for the two jets in

TABLE I. Leptonic cuts on the leptonic decay products of the diboson channels:  $W^+W^-$ ,  $W^\pm W^\pm$ ,  $W^\pm Z$ , and  $ZZ$ .

$W^+W^-$	$W^\pm W^\pm$	$W^\pm Z$	$ZZ$
$p_{T_\ell} > 100$ GeV	$p_{T_\ell} > 100$ GeV	$p_{T_\ell} > 100$ GeV	$p_{T_\ell} > 50$ GeV
$ y_\ell  < 2$	$ y_\ell  < 2$	$ y_\ell  < 2$	$ y_\ell  < 2$
$M_{\ell^+\ell^-} > 250$ GeV	$M_{\ell^\pm\ell^\pm} > 250$ GeV	$M_{3\ell} > 375$ GeV	$M_{4\ell} > 500$ GeV

selecting the VBF events:

$$E_{T_{j1,j2}} > 30 \text{ GeV}, \quad |\eta_{j1,j2}| < 4.7, \quad \Delta\eta_{12} = |\eta_{j1} - \eta_{j2}| > 3.5, \quad \eta_{j1}\eta_{j2} < 0, \quad (8)$$

where  $E_{T_{j1,j2}}$  and  $\eta_{j1,j2}$  are the transverse energies and pseudo-rapidities respectively of the two forward jets, and

$$M_{jj} > 500 \text{ GeV} \quad (9)$$

on their invariant mass  $M_{jj}$  at  $\sqrt{s} = 13$  TeV. This set of cuts is more or less the same as those used by CMS [19] and ATLAS [20] in their searches for fermiophobic Higgs boson using VBF. The cuts for the leptonic decay modes  $W \rightarrow \ell\nu_\ell$  and  $Z \rightarrow \ell^+\ell^-$  for each of the  $W^+W^-$ ,  $W^\pm W^\pm$ ,  $W^\pm Z$ , and  $ZZ$  channels are slightly different, which we list separately in Table I. We sum over the charged leptons  $\ell = e, \mu$ .

We set the mass of the heavier CP-even Higgs boson to be 2 TeV, which basically at the margin of the LHC reach. The charged and the CP-odd Higgs bosons are not relevant to the  $WW$  scattering here. Therefore, the only relevant parameter to this study is  $\sin(\beta - \alpha)$ , which we shall use 0.5, 0.7, 0.9 as illustrations.

We use MADGRAPH 5 [21] to perform the full parton-level calculations, including the decays of the  $W$  and  $Z$  bosons. Then we turn on PYTHIA 8.1 [22] for parton showering and jet radiation, and use PYTHIA-PGS [23] to perform detector simulation to provide jet and lepton reconstruction.

We expect that the enhancement in the differential cross section in the large invariant-mass region of the vector-boson pair will be manifested at the large invariant-mass of its decay products, e.g.,  $M_{\ell\ell}$  in both  $W^\pm W^\pm$  and  $W^+W^-$  channels, and  $M_{3\ell}$  and  $M_{4\ell}$  in  $WZ$  and  $ZZ$  channels, respectively (see Table I). We show the invariant-mass distributions of the charged leptons in various diboson channels  $W^+W^-$ ,  $W^+W^+$ ,  $W^+Z$ ,  $ZZ$  for  $\sin(\beta - \alpha) =$

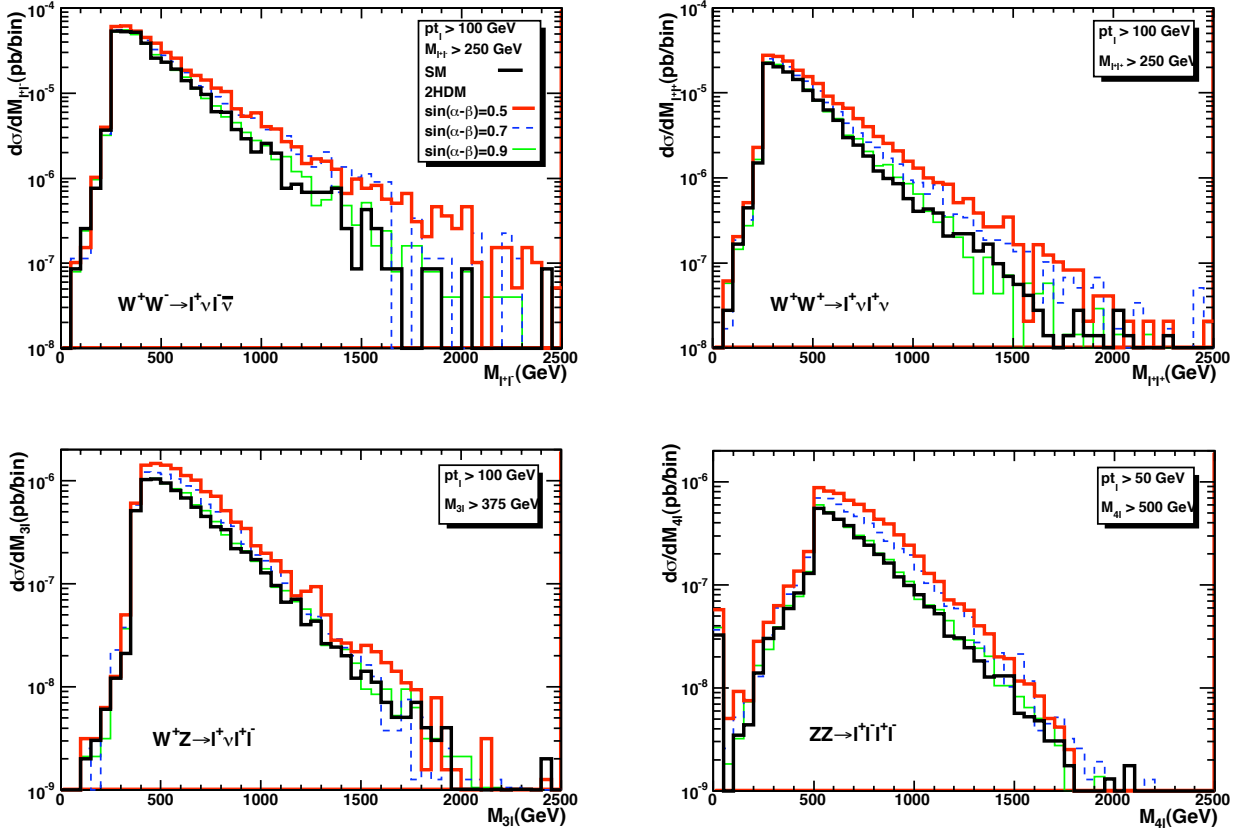


FIG. 1. Invariant-mass distributions of the charged leptons in various diboson channels  $W^+W^-$ ,  $W^+W^+$ ,  $W^+Z$ ,  $ZZ$  for  $\sin(\beta - \alpha) = 0.5, 0.7, 0.9$ .

0.5, 0.7, 0.9 as well as the SM in Fig. 1. In the figures, we show only  $W^+W^+$  and  $W^+Z$  channels since  $W^-W^-$  and  $W^-Z$  are relatively smaller. In Table II, we show the cross sections for all channels after the leptonic and jet cuts in various diboson channels for  $\sin(\beta - \alpha) = 0.5, 0.7, 0.9$  and the SM.

The difference between the cross section of the SM and the one with  $\sin(\beta - \alpha) \neq 1$  is the signal of enhancement due to the deviation in the  $g_{hWW}$  coupling. The largest enhancement happens in the  $W^+W^-$  and  $ZZ$  channels. In the  $W^+W^-$  channel, the enhancement is  $(0.51 - 0.39)/0.39 \approx 0.31$  and  $(0.46 - 0.39)/0.39 \approx 0.18$  for  $\sin(\beta - \alpha) = 0.5$  and 0.7, respectively; while in the  $ZZ$  channel the enhancement is  $(8.4 - 4.4) \times 10^{-3}/4.4 \times 10^{-3} = 0.91$  and  $(6.4 - 4.4) \times 10^{-3}/4.4 \times 10^{-3} = 0.45$  for  $\sin(\beta - \alpha) = 0.5$  and 0.7, respectively. Because of the overall smallness of the  $ZZ$  channel compared with other channels, even if we can collect the planned  $300 \text{ fb}^{-1}$  luminosity at the LHC, the event rate for  $ZZ \rightarrow 4\ell$  is too

TABLE II. Cross sections in fb in various diboson channels under the jet cuts in Eqs. (8) and (9), and leptonic cuts listed in Table I.

Channels	Cross Sections (fb)			
	$\sin(\beta - \alpha) = 0.5$	0.7	0.9	SM ( $C_v = 1$ )
$W^+W^- \rightarrow \ell^+\nu\ell^-\bar{\nu}$	0.51	0.46	0.40	0.39
$W^+W^+ \rightarrow \ell^+\nu\ell^+\nu$	0.20	0.17	0.14	0.14
$W^-W^- \rightarrow \ell^-\bar{\nu}\ell^-\bar{\nu}$	0.083	0.075	0.070	0.069
$W^+Z \rightarrow \ell^+\nu\ell^+\ell^-$	0.016	0.013	0.011	0.010
$W^-Z \rightarrow \ell^-\bar{\nu}\ell^+\ell^-$	$1.0 \times 10^{-2}$	$8.5 \times 10^{-3}$	$7.6 \times 10^{-3}$	$7.4 \times 10^{-3}$
$ZZ \rightarrow \ell^+\ell^-\ell^+\ell^-$	$8.4 \times 10^{-3}$	$6.4 \times 10^{-3}$	$4.6 \times 10^{-3}$	$4.4 \times 10^{-3}$

small for detection. On the other hand, the event rate for  $W^+W^- \rightarrow 2\ell 2\nu$  is sufficient for detection at the LHC.

#### IV. CONCLUSION

In this work, we have demonstrated that detailed studies of longitudinal weak gauge boson scattering at the LHC can provide useful hints of new physics at a higher scale, despite only a light Higgs boson has been discovered at the LHC. If unitarity is only partially fulfilled by the light Higgs boson, the  $WW$  scattering cross sections must be growing as energy increases before it reaches the other heavier Higgs bosons or other UV completion to achieve the full unitarization. This partial and temporary growth of the cross sections can be palpable at the LHC provided that the UV part resides at a sufficiently high scale. On the other hand, if the UV part is within the reach of the LHC energies, the  $WW$  scattering can also reveal it as a bump in the invariant mass distribution. This can be realized in a number of multi-Higgs-doublet models, e.g, 2HDM. Our approach of using longitudinal weak gauge boson scattering is more direct and perhaps more efficient to probe the EWSB. Partial growth in the  $WW$  scattering cross sections can be a generic feature in many extensions of the SM. Detection of such a behavior at the LHC would be fascinating. Perhaps Higgs is not a lone player.

*Acknowledgments.* This work was supported in part by the National Science Council of Taiwan under two grants 99-2112-M-007-005-MY3 and 101-2112-M-001-005-MY3 as well as the WCU program through the KOSEF funded by the MEST (R31-2008-000-10057-0).

---

- [1] G. Aad *et al.* [ATLAS Collaboration], “son with the ATLAS detector at the LHC,” *Phys. Lett. B* **716**, 1 (2012) [arXiv:1207.7214 [hep-ex]].
- [2] S. Chatrchyan *et al.* [CMS Collaboration], “the LHC,” *Phys. Lett. B* **716**, 30 (2012) [arXiv:1207.7235 [hep-ex]].
- [3] P. W. Higgs, *Phys. Rev. Lett.* **13**, 508 (1964); F. Englert and R. Brout, *Phys. Rev. Lett.* **13**, 321 (1964); G. S. Guralnik, C. R. Hagen and T. W. B. Kibble, *Phys. Rev. Lett.* **13**, 585 (1964).
- [4] See, e.g., K. Cheung, J. S. Lee and P. -Y. Tseng, arXiv:1302.3794 [hep-ph].
- [5] See, e.g., S. Chang, S. K. Kang, J. -P. Lee, K. Y. Lee, S. C. Park and J. Song, arXiv:1210.3439 [hep-ph]; C. -Y. Chen and S. Dawson, arXiv:1301.0309 [hep-ph]; A. Celis, V. Ilisie and A. Pich, arXiv:1302.4022 [hep-ph].
- [6] G. F. Giudice, C. Grojean, A. Pomarol and R. Rattazzi, *JHEP* **0706**, 045 (2007).
- [7] B. W. Lee, C. Quigg and H. B. Thacker, *Phys. Rev. D* **16**, 1519 (1977); M. S. Chanowitz, *Czech. J. Phys.* **55**, B45 (2005).
- [8] Y. P. Yao and C. P. Yuan, *Phys. Rev. D* **38**, 2237 (1988); H. G. J. Veltman, *Phys. Rev. D* **41**, 2294 (1990); H. J. He, Y. P. Kuang and X. Y. Li, *Phys. Rev. Lett.* **69**, 2619 (1992).
- [9] K. Cheung, C. -W. Chiang and T. -C. Yuan, *Phys. Rev. D* **78**, 051701 (2008) [arXiv:0803.2661 [hep-ph]].
- [10] K. Cheung, C. -W. Chiang, Y. -K. Hsiao and T. -C. Yuan, *Phys. Rev. D* **81**, 053001 (2010) [arXiv:0911.0734 [hep-ph]].
- [11] S. Dawson, *Nucl. Phys. B* **249**, 42 (1985).
- [12] V. D. Barger, K. -m. Cheung, T. Han and D. Zeppenfeld, *Phys. Rev. D* **44**, 2701 (1991) [Erratum-*ibid.* *D* **48**, 5444 (1993)]; V. D. Barger, K. -m. Cheung, T. Han, J. Ohnemus and D. Zeppenfeld, *Phys. Rev. D* **44**, 1426 (1991).
- [13] V. D. Barger, K. -m. Cheung, T. Han and R. J. N. Phillips, *Phys. Rev. D* **42**, 3052 (1990).
- [14] J. Bagger *et al.*, *Phys. Rev. D* **49**, 1246 (1994); *ibid.* **52**, 3878 (1995).

- [15] B. Zhang, Y. -P. Kuang, H. -J. He and C. P. Yuan, Phys. Rev. D **67**, 114024 (2003) [hep-ph/0303048].
- [16] T. Han, D. Krohn, L. -T. Wang and W. Zhu, JHEP **1003**, 082 (2010) [arXiv:0911.3656 [hep-ph]].
- [17] G. Degrandi, S. Di Vita, J. Elias-Miro, J. R. Espinosa, G. F. Giudice, G. Isidori and A. Strumia, JHEP **1208**, 098 (2012) [arXiv:1205.6497 [hep-ph]].
- [18] T. Hambye and K. Riessmann, Phys. Rev. D **55**, 7255 (1997) [hep-ph/9610272].
- [19] CMS Collaboration, CMS-PAS-HIG-12-002.
- [20] ATLAS Collaboration, ATLAS-CONF-2012-13.
- [21] MADGRAPH: J. Alwall, M. Herquet, F. Maltoni, O. Mattelaer and T. Stelzer, “*MadGraph 5 : Going Beyond*,” JHEP **1106**, 128 (2011) [arXiv:1106.0522 [hep-ph]].
- [22] T. Sjostrand, S. Mrenna and P. Z. Skands, “*A Brief Introduction to PYTHIA 8.1*,” Comput. Phys. Commun. **178**, 852 (2008) [arXiv:0710.3820 [hep-ph]].
- [23] J. Alwall and the CP3 development team, *The MG/ME Pythia-PGS package*; the Madgraph at <http://madgraph.hep.uiuc.edu/>; Pythia at <https://pythia6.hepforge.org/>; and PGS at <http://www.physics.ucdavis.edu/~conway/research/software/pgs/pgs4-general.htm>.